Kaons and antikaons in hot and dense hadronic matter

A. Mishra,* E. L. Bratkovskaya,† J. Schaffner-Bielich, S. Schramm, and H. Stöcker
Institut für Theoretische Physik, J. W. Goether Universität, Robert Mayer Strasse 8-10, D-60054 Frankfurt am Main, Germany
(Received 18 February 2004; published 14 October 2004)

The medium modification of kaon and antikaon masses, compatible with low-energy kaon-nucleon scattering data, are studied in a chiral SU(3) model. The mutual interactions with baryons in hot hadronic matter and the effects from the baryonic Dirac sea on the $K(\bar{K})$ masses are examined. The in-medium masses from the chiral SU(3) effective model are compared to those from chiral perturbation theory. Furthermore, the influence of these in-medium effects on kaon rapidity distributions and transverse energy spectra, as well as the $K,\bar{K}$ flow pattern in heavy-ion collision experiments at 1.5–2 *A* GeV are investigated within the hadron-string-dynamics transport approach. Detailed predictions on the transverse momentum and rapidity dependence of directed flow v_1 and the elliptic flow v_2 are provided for Ni+Ni at 1.93*A* GeV within the various models, that can be used to determine the in-medium $K^{\pm}$ properties from the experimental side in the near future.

DOI: 10.1103/PhysRevC.70.044904 PACS number(s): 24.10.Cn, 25.75.−q, 13.75.Jz

I. INTRODUCTION

The property of hadrons under extreme conditions of temperature and density [1] is an important topic in present strong-interaction physics. This subject has direct implications in heavy-ion collision experiments, in the study of astrophysical compact objects (like neutron stars), as well as in the early universe. The in-medium properties of kaons have been primarily investigated due to their relevance in neutron star phenomenology as well as relativistic heavy-ion collisions. For example, in the interior of the neutron star, the attractive kaon nucleon interaction might lead to kaon condensation as suggested early by Kaplan and Nelson [2]. The in-medium modification of kaon/antikaon properties can be observed experimentally primarily in relativistic nuclear collisions. Indeed, the experimental [3–7] and theoretical studies [8–19] on $K^{\pm}$ production from $A+A$ collisions at Schwer-Ionen-Synchrotron (SIS) energies of 1–2 *A* GeV have shown that in-medium properties of kaons have been seen in the collective flow pattern of K^+ mesons [20] as well as in the abundancy and spectra of antikaons.

The theoretical research work on the topic of in-medium properties of hadrons was triggered in part by the early suggestion of Brown and Rho [21], that the modifications of hadron masses should scale with the scalar quark condensate $\langle q\bar{q}\rangle$ at finite baryon density. The first attempts to extract the antikaon-nucleus potential from the analysis of kaonic-atom data were in favor of very strong attractive potentials of the order of -150 to -200 MeV at normal nuclear matter density ρ_0 [22,23]. However, more recent self-consistent calculations based on a chiral Lagrangian [24–27] or coupled-channel *G*-matrix theory (within meson-exchange potentials) [29] only predicted moderate attractive depths of -50 to -80 MeV at density ρ_0.

The problem with the antikaon potential at finite baryon density is that the antikaon-nucleon amplitude in the isospin channel $I=0$ is dominated by the $\Lambda(1405)$ resonant structure [28], which in free space is only 27 MeV below the $\bar{K}N$ threshold. It is presently not clear if this physical resonance is a real excited state of a "strange" baryon or it is some short-lived intermediate state which can be generated dynamically in a coupled-channel *T*-matrix scattering equation using a suitable meson-baryon potential. Additionally, the coupling between the $\bar{K}N$ and πY $(Y=\Lambda,\Sigma)$ channels is essential to get the proper dynamical behavior in free space. Correspondingly, the in-medium properties of the $\Lambda(1405)$, such as its pole position and its width, which in turn strongly influence the antikaon-nucleus optical potential, are very sensitive to the many-body treatment of the medium effects. Previous works have shown that a self-consistent treatment of the $\bar{K}$ self-energy has a strong impact on the scattering amplitudes [17,24,26,27,29,30] and thus on the in-medium properties of the antikaon. Due to the complexity of this many-body problem, the actual kaon and antikaon self-energies (or potentials) are still a matter of debate.

In the present investigation, we will use a chiral SU(3) model for the description of hadrons in the medium [31]. The nucleons—as modified in the hot hyperonic matter—have been studied within this model [32] previously. Furthermore, the properties of vector mesons [32,33]—due to their interactions with nucleons in the medium—have been also examined and have been found to show appreciable modifications due to Dirac sea polarization effects. The chiral $SU(3)_{\text{flavor}}$ model was also been generalized to $SU(4)_{\text{flavor}}$ to study the mass modification of *D* mesons due to their interactions with the light hadrons in hot hadronic matter in [34]. In the present work, the masses of kaons (antikaons), as modified in the medium due to their interaction with nucleons, are studied within the chiral SU(3) framework, which is consistent with the low-energy kaon-nucleon (KN) scattering data [35]. In this approach, however, only the real parts of the kaon/antikaon self-energies can be addressed.

Another problem related to the complexity of kaon/antikaon physics in relativistic heavy-ion reactions is that not only the mean-field properties of the $K,\bar{K}$ mesons enter, but

*Electronic address: mishra@th.physik.uni-frankfurt.de
†Electronic address: Elena.Bratkovskaya@th.physik.uni-frankfurt.de

also their in-medium scattering amplitudes sometimes far from the mass shell [16,29], because the antikaon couples strongly to the baryons and achieves a nontrivial spectral width in the medium. Whereas in the early calculations in Refs. [10–15] the off-shell transition amplitudes have been simply extrapolated from on-shell cross sections in vacuum, more recent studies in Ref. [16] have incorporated the full off-shell dynamics in transport. Thus, when confronting our model predictions with experimental data, we will use a parametrization of the off-shell amplitudes from Refs. [16,29] in order to reduce the systematic uncertainty in the transition amplitudes or scattering rates of antikaons with baryons. For the real part of the self-energies, however, we will implement the results from the different models to be discussed in this work.

The outline of the paper is as follows: In Sec. II we shall briefly recall the basic concepts of the chiral SU(3) model used in the present investigation. Section III describes the medium modification of the $K(\bar{K})$ mesons in this effective model. In Sec. IV, we investigate the kaon masses using chiral perturbation theory, while in Sec. V we discuss and compare the results from the chiral SU(3) model to those from the chiral perturbation theory. Section VI explores the effects of in-medium modifications of kaons (antikaons) on their production and flow pattern in relativistic heavy-ion collisions in comparison to experimental data. Section VII summarizes the findings of the present investigation and discusses future extensions.

II. THE HADRONIC CHIRAL SU(3)×SU(3) MODEL

In this section the various terms of the effective hadronic Lagrangian used,

$$\mathcal{L} = \mathcal{L}_{kin} + \sum_{W=X,Y,V,A,u} \mathcal{L}_{BW} + \mathcal{L}_{VP} + \mathcal{L}_{vec} + \mathcal{L}_0 + \mathcal{L}_{SB}, \quad (1)$$

are briefly reviewed. Equation (1) corresponds to a relativistic quantum-field-theoretical model of baryons and mesons built on a nonlinear realization of chiral symmetry and broken scale invariance (for details, see [31–33]) to describe strongly interacting nuclear matter. The model was used successfully to describe nuclear matter, finite nuclei, hypernuclei, and neutron stars. The Lagrangian contains the baryon octet, the spin-0 and spin-1 meson multiplets as the elementary degrees of freedom. In Eq. (1), $\mathcal{L}_{kin}$ is the kinetic energy term, $\mathcal{L}_{BW}$ contains the baryon-meson interactions in which the baryon-spin-0 meson interaction terms generate the baryon masses. $\mathcal{L}_{VP}$ describes the interactions of vector mesons with the pseudoscalar mesons (and with photons). $\mathcal{L}_{vec}$ describes the dynamical mass generation of the vector mesons via couplings to the scalar mesons and contains additionally quartic self-interactions of the vector fields. $\mathcal{L}_0$ contains the meson-meson interaction terms inducing the spontaneous breaking of chiral symmetry as well as a scale invariance breaking logarithmic potential. $\mathcal{L}_{SB}$ describes the explicit chiral symmetry breaking.

The kinetic energy terms are given as

$$\mathcal{L}_{kin} = i\,\mathrm{Tr}\,\bar{B}\gamma_\mu D^\mu B + \frac{1}{2}\mathrm{Tr}\,D_\mu X D^\mu X + \mathrm{Tr}(u_\mu X u^\mu X + X u_\mu u^\mu X) + \frac{1}{2}\mathrm{Tr}\,D_\mu Y D^\mu Y + \frac{1}{2}D_\mu \chi D^\mu \chi - \frac{1}{4}\mathrm{Tr}(\tilde{V}_{\mu\nu}\tilde{V}^{\mu\nu}) - \frac{1}{4}\mathrm{Tr}(F_{\mu\nu}F^{\mu\nu}) - \frac{1}{4}\mathrm{Tr}(\mathcal{A}_{\mu\nu}\mathcal{A}^{\mu\nu}). \quad (2)$$

In Eq. (2), B is the baryon octet, X the scalar meson multiplet, Y the pseudoscalar chiral singlet, $\tilde{V}^\mu(\mathcal{A}^\mu)$ the renormalized vector (axial vector) meson multiplet with the field strength tensor $\tilde{V}_{\mu\nu}=\partial_\mu\tilde{V}_\nu-\partial_\nu\tilde{V}_\mu(\mathcal{A}_{\mu\nu}=\partial_\mu\mathcal{A}_\nu-\partial_\nu\mathcal{A}_\mu)$, $F_{\mu\nu}$ is the field strength tensor of the photon and χ is the scalar, isoscalar dilaton (glueball) field. In the above, $u_\mu=-i/2[u^\dagger\partial_\mu u-u\partial_\mu u^\dagger]$, where $u=\exp[(i/\sigma_0)\pi^a\lambda^a\gamma_5]$ is the unitary transformation operator, and the covariant derivative reads $D_\mu=\partial_\mu+[\Gamma_\mu,]$ with $\Gamma_\mu=-i/2[u^\dagger\partial_\mu u+u\partial_\mu u^\dagger]$.

The baryon-meson interaction for a general meson field W has the form

$$\mathcal{L}_{BW} = -\sqrt{2}g_8^W\{\alpha_W[\bar{B}\mathcal{O}BW]_F + (1-\alpha_W)[\bar{B}\mathcal{O}BW]_D\} - g_1^W\frac{1}{\sqrt{3}}\mathrm{Tr}(\bar{B}\mathcal{O}B)\mathrm{Tr}\,W, \quad (3)$$

with $[\bar{B}\mathcal{O}BW]_F := \mathrm{Tr}(\bar{B}\mathcal{O}WB-\bar{B}\mathcal{O}BW)$ and $[\bar{B}\mathcal{O}BW]_D := \mathrm{Tr}(\bar{B}\mathcal{O}WB+\bar{B}\mathcal{O}BW)-(2/3)\mathrm{Tr}(\bar{B}\mathcal{O}B)\mathrm{Tr}\,W$. The different terms—to be considered—are those for the interaction of baryons with scalar mesons ($W=X,\mathcal{O}=1$), with vector mesons ($W=\tilde{V}_\mu,\mathcal{O}=\gamma_\mu$ for the vector and $W=\tilde{V}_{\mu\nu},\mathcal{O}=\sigma^{\mu\nu}$ for the tensor interaction), with axial vector mesons ($W=\mathcal{A}_\mu,\mathcal{O}=\gamma_\mu\gamma_5$ and with pseudoscalar mesons ($W=u_\mu,\mathcal{O}=\gamma_\mu\gamma_5$), respectively. For the current investigation the following interactions are relevant: Baryon-scalar meson interactions generate the baryon masses through coupling of the baryons to the nonstrange $\sigma(\sim\langle\bar{u}u+\bar{d}d\rangle)$ and the strange $\zeta(\sim\langle\bar{s}s\rangle)$ scalar quark condensate. The parameters g_1^S, g_8^S, and α_S are adjusted to fix the baryon masses to their experimentally measured vacuum values. It should be emphasized that the nucleon mass also depends on the strange condensate ζ. For the special case of ideal mixing ($\alpha_S=1$ and $g_1^S=\sqrt{6}g_8^S$) the nucleon mass depends only on the nonstrange quark condensate. In the present investigation, the general case will be used to study hot and strange hadronic matter [32], which takes into account the baryon coupling terms to both scalar fields (σ and ζ) while summing over the baryonic tadpole diagrams to investigate the effect from the baryonic Dirac sea in the relativistic Hartree approximation [32].

In analogy to the baryon-scalar meson coupling there exist two independent baryon-vector meson interaction terms corresponding to the F-type (antisymmetric) and D-type (symmetric) couplings. Here we will use the antisymmetric coupling because—from the universality principle [36] and the vector meson dominance model—one can conclude that the symmetric coupling should be small. We realize it by setting $\alpha_V=1$ for all fits. Additionally we decouple the

strange vector field $\phi_\mu \sim \bar{s}\gamma_\mu s$ from the nucleon by setting $g_1^V = \sqrt{6} g_8^V$. The remaining baryon-vector meson interaction reads

$$\mathcal{L}_{BV} = -\sqrt{2} g_8^V \{[\bar{B}\gamma_\mu B V^\mu]_F + \mathrm{Tr}(\bar{B}\gamma_\mu B)\mathrm{Tr}\, V^\mu\}. \quad (4)$$

The Lagrangian describing the interaction for the scalar mesons X and pseudoscalar singlet Y is given as [31]

$$\mathcal{L}_0 = -\frac{1}{2}k_0\chi^2 I_2 + k_1(I_2)^2 + k_2 I_4 + 2k_3\chi I_3, \quad (5)$$

with $I_2 = \mathrm{Tr}(X+iY)^2$, $I_3 = \det(X+iY)$, and $I_4 = \mathrm{Tr}(X+iY)^4$. In the above, χ is the scalar color singlet gluon field. It is introduced in order to "mimic" the QCD trace anomaly, i.e., the nonvanishing energy-momentum tensor $\theta_\mu^\mu = (\beta_{\mathrm{QCD}}/2g)\langle G_{\mu\nu}^a G^{a,\mu\nu}\rangle$, where $G_{\mu\nu}^a$ is the gluon field tensor. The following scale breaking potential is introduced

$$\mathcal{L}_{\mathrm{scalebreak}} = -\frac{1}{4}\chi^4 \ln\frac{\chi^4}{\chi_0^4} + \frac{\delta}{3}\chi^4 \ln\frac{I_3}{\det\langle X\rangle_0}, \quad (6)$$

which allows for the identification of the χ field width the gluon condensate $\theta_\mu^\mu = (1-\delta)\chi^4$. Finally the term $\mathcal{L}_\chi = -k_4\chi^4$ generates a phenomenologically consistent finite vacuum expectation value. The variation of χ in the medium is rather small [31]. Hence, we shall use the frozen glueball approximation, i.e., set χ to its vacuum value, χ_0.

The Lagrangian for the vector meson interaction is written as

$$\mathcal{L}_{vec} = \frac{m_V^2}{2}\frac{\chi^2}{\chi_0^2}\mathrm{Tr}(\tilde{V}_\mu\tilde{V}^\mu) + \frac{\mu}{4}\mathrm{Tr}(\tilde{V}_{\mu\nu}\tilde{V}^{\mu\nu}X^2) + \frac{\lambda_V}{12}[\mathrm{Tr}(\tilde{V}^{\mu\nu})]^2 + 2(\tilde{g}_4)^4\mathrm{Tr}(\tilde{V}_\mu\tilde{V}^\mu)^2. \quad (7)$$

The vector meson fields, $\tilde{V}_\mu$ are related to the renormalized fields by $V_\mu = Z_V^{1/2}\tilde{V}_\mu$, with $V = \omega, \rho, \phi$. The masses of ω, ρ, and ϕ are fitted from m_V, μ, and λ_V.

The explicit symmetry-breaking term is given as [31]

$$\mathcal{L}_{SB} = \mathrm{Tr}\, A_p[u(X+iY)u + u^\dagger(X-iY)u^\dagger], \quad (8)$$

with $A_p = 1/\sqrt{2}\,\mathrm{diag}(m_\pi^2 f_\pi, m_\pi^2 f_\pi, 2m_K^2 f_K - m_\pi^2 f_\pi)$ and $m_\pi = 139$ MeV, $m_K = 498$ MeV. This choice for A_p, together with the constraints $\sigma_0 = -f_\pi$, $\zeta_0 = -1/\sqrt{2}(2f_K - f_\pi)$ on the vacuum expectation value (VEV) on the scalar condensates assure that the partially conserved axial-vector current (PCAC) relations of the pion and kaon are fulfilled. With $f_\pi = 93.3$ MeV and $f_K = 122$ MeV we obtain $|\sigma_0| = 93.3$ MeV and $|\zeta_0| = 106.56$ MeV.

We will treat the chiral SU(3) model in the mean field and in the relativistic Hartree approximations (for details, we refer to Refs. [32,33]).

III. KAON INTERACTIONS IN THE EFFECTIVE CHIRAL MODEL

In this section, we investigate the medium modification of the K-meson mass due to the interactions of the K mesons in the hadronic medium. In the chiral effective model as used here, the interactions to the scalar fields (nonstrange, σ and strange, ζ) as well as a vectorial interaction and a ω-exchange term modify the masses for $K^\pm$ mesons in the medium. These interactions were considered within the SU(3) chiral model to investigate the modifications of K mesons in the thermal medium [37] in the mean-field approximation. The scalar meson exchange gives an attractive interaction leading to a drop of the K-meson masses similar to a scalar sigma term in the chiral perturbation theory [2]. In fact, the KN [37] as well as the πN sigma term are predicted in our approach automatically by using SU(3) symmetry. The pion-nucleon and kaon-nucleon sigma terms, as calculated from the scalar meson exchange interaction of our Lagrangian, are 28 and 463 MeV, respectively. The value for the KN sigma term calculated in our model is close to the value of $\Sigma_{KN} = 450$ MeV found by lattice gauge calculations [38]. In addition to the terms considered in [37], we also account the effect of repulsive scalar contributions $[\sim(\partial_\mu K^+)(\partial^\mu K^-)]$, which contribute in the same order as the attractive sigma term in chiral perturbation theory. These terms will ensure that KN scattering lengths can be described and, hence, the low-density theorem for kaons is fulfilled.

The scalar meson multiplet has the expectation value $\langle X\rangle = \mathrm{diag}(\sigma/\sqrt{2}, \sigma/\sqrt{2}, \zeta)$, with σ and ζ corresponding to the nonstrange and strange scalar condensates. The pseudoscalar meson field P can be written as,

$$P = \begin{pmatrix} \pi^0/\sqrt{2} & \pi^+ & \dfrac{2K^+}{1+w} \\ \pi^- & -\pi^0/\sqrt{2} & 0 \\ \dfrac{2K^-}{1+w} & 0 & 0 \end{pmatrix}, \quad (9)$$

where $w = \sqrt{2}\zeta/\sigma$, and we have written down the entries which are relevant for the present investigation. From PCAC, one gets the decay constants for the pseudoscalar mesons as $f_\pi = -\sigma$ and $f_K = -(\sigma + \sqrt{2}\zeta)/2$. The vector meson interaction with the pseudoscalar mesons, which modifies the masses of the K mesons, is given as [37]

$$\mathcal{L}_{VP} = -\frac{m_V^2}{2g_V}\mathrm{Tr}(\Gamma_\mu V^\mu) + \mathrm{h.c.}. \quad (10)$$

The vector meson multiplet is given as $V = \mathrm{diag}[(\omega + \rho_0)/\sqrt{2}, (\omega - \rho_0)/\sqrt{2}, \phi]$. The non-diagonal components in the multiplet, which are not relevant in the present investigation, are not written down. With the interaction (10), the coupling of the K meson to the ω meson is related to the pion-rho coupling as $g_{\omega K}/g_{\rho\pi\pi} = f_\pi^2/(2f_K^2)$.

The scalar meson exchange interaction term, which is attractive for the K mesons, is given from the explicit symmetry-breaking term by Eq. (8), where $A_p = 1/\sqrt{2}\,\mathrm{diag}(m_\pi^2 f_\pi, m_\pi^2 f_\pi, 2m_K^2 f_K - m_\pi^2 f_\pi)$.

The interaction Lagrangian modifying the K-meson mass can be written as [37]

$$\mathcal{L}_K = -\frac{3i}{8f_K^2}\bar{N}\gamma^\mu N(K^-\partial_\mu K^+ - \partial_\mu K^- K^+) + \frac{m_K^2}{2f_K}(\sigma+\sqrt{2}\zeta)K^-K^+$$
$$- ig_{\omega K}(K^-\partial_\mu K^+ - \partial_\mu K^- K^+)\omega^\mu - \frac{1}{f_K}(\sigma+\sqrt{2}\zeta)(\partial_\mu K^-)$$
$$\times(\partial^\mu K^+) + \frac{d_1}{2f_K^2}(\bar{N}N)(\partial_\mu K^-)(\partial^\mu K^+). \quad (11)$$

In Eq. (11) the first term is the vectorial interaction term obtained from the first term in Eq. (2) (Weinberg-Tomozawa term). The second term, which gives an attractive interaction for the K mesons, is obtained from the explicit symmetry-breaking term (8). The third term, referring to the interaction in terms of ω-meson exchange, is attractive for the K^- and repulsive for K^+. The fourth term arises within the present chiral model from the kinetic term of the pseudoscalar mesons given by the third term in Eq. (2), when the scalar fields in one of the meson multiplets, X are replaced by their vacuum expectation values. The fifth term in Eq. (11) for the KN interactions arises from the term

$$\mathcal{L}^{BM} = d_1\,\mathrm{Tr}(u_\mu u^\mu \bar{B}B), \quad (12)$$

in the SU(3) chiral model. The last two terms in Eq. (11) represent the range term in the chiral model. From the Fourier transformation of the equation of motion for kaons

$$-\omega^2 + m_K^2 + \Sigma_K(\omega,\rho) = 0,$$

one derives the effective energy of the K^+ and K^-, which are the poles of the kaon propagator in the medium (assuming zero momentum for S-wave Bose condensation), where Σ_K denotes the kaon self-energy in the medium.

Fitting to KN scattering data

For the KN interactions, the term (12) reduces to

$$\mathcal{L}_{\tilde{D}}^{KN} = d_1\frac{1}{2f_K^2}(\bar{N}N)(\partial_\mu K^-)(\partial^\mu K^+). \quad (13)$$

The coefficient d_1 in the above is determined by fitting to the KN scattering length [34,35,39,40]. The isospin averaged KN scattering length

$$\bar{a}_{KN} = \frac{1}{4}(3a_{KN}^{I=1} + a_{KN}^{I=0}) \quad (14)$$

can be calculated to be

$$\bar{a}_{KN} = \frac{m_K}{4\pi(1+m_K/m_N)}\left[-\left(\frac{m_K}{2f_K}\right)\cdot\frac{g_{\sigma N}}{m_\sigma^2} - \left(\frac{\sqrt{2}m_K}{2f_K}\right)\cdot\frac{g_{\zeta N}}{m_\zeta^2}\right.$$
$$\left. - \frac{2g_{\omega K}g_{\omega N}}{m_\omega^2} - \frac{3}{4f_K^2} + \frac{d_1 m_K}{2f_K^2}\right]. \quad (15)$$

The empirical value of the isospin averaged scattering length [35,39,40] is taken to be

$$\bar{a}_{KN} \approx -0.255\ \mathrm{fm}, \quad (16)$$

which determines the value for the coefficient d_1. The present calculations use the values, $g_{\sigma N}=10.618$ and $g_{\zeta N}=-0.4836$ as fixed by the vacuum baryon masses, and the other parameters are fitted to the nuclear matter saturation properties as listed in Ref. [32]. We consider the case when a quartic vector interaction is present. The coefficient d_1 is evaluated in the mean-field and relativistic Hartree approximation (RHA) cases as $5.63/m_K$ and $4.33/m_K$, respectively [34]. The contribution from this term is thus seen to be attractive, contrary to the other term proportional to $(\partial_\mu K^-)(\partial^\mu K^+)$ in Eq. (11), which is repulsive.

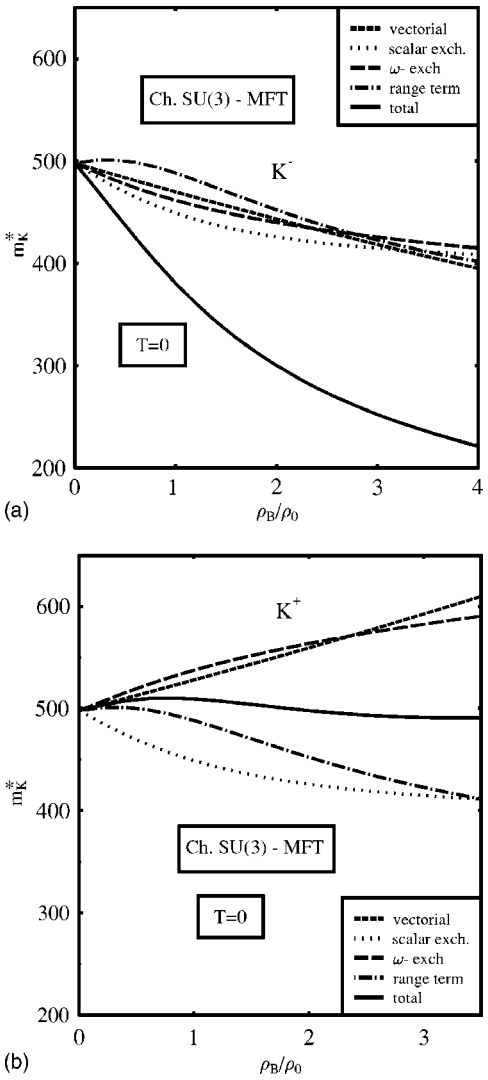

FIG. 1. Contributions to the masses of $K^\pm$ mesons due to the various interactions in the effective chiral model in the mean-field approximation. The curves refer to individual contributions from the vectorial interaction, scalar exchange, ω exchange, and the range term. The solid line shows the total contribution.

IV. CHIRAL PERTURBATION THEORY

The effective Lagrangian obtained from chiral perturbation theory [2] has been used extensively in the literature for the study of kaons in dense matter. This approach has a vector interaction (called the Tomozawa-Weinberg term) as the leading term. At subleading order there are the attractive sca-

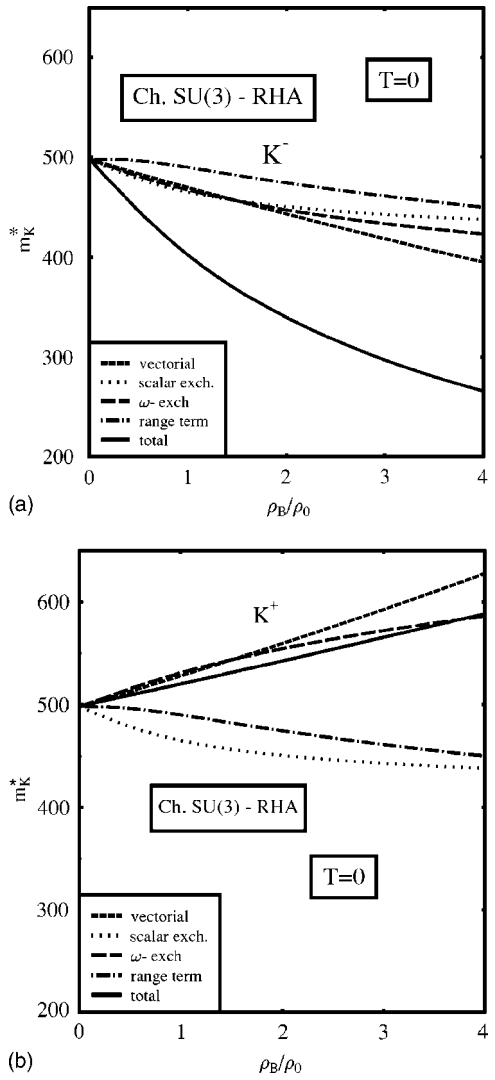

FIG. 2. Same as in Fig. 1, but in the relativistic Hartree approximation. The contributions to the masses of $K^{\pm}$ mesons due to the various interactions are seen to be smaller with the Dirac sea effects.

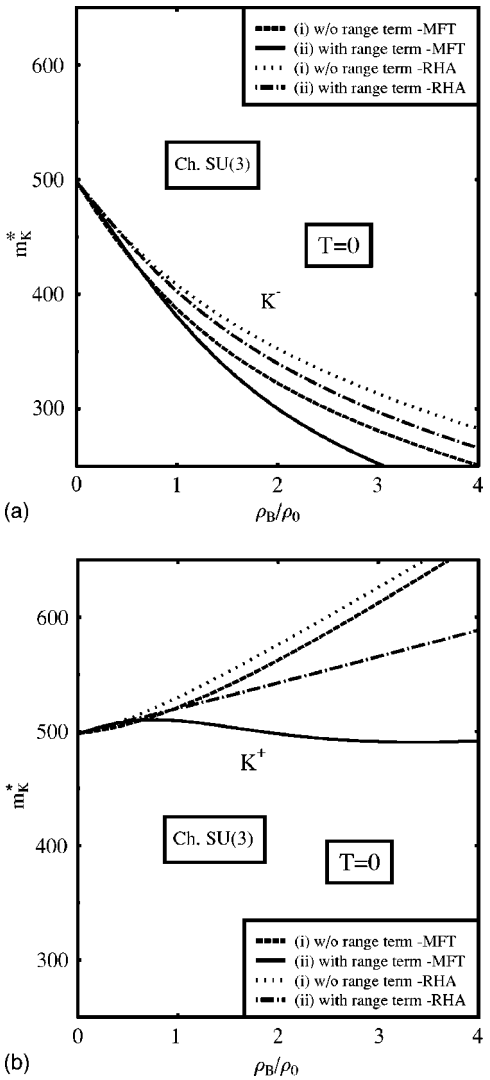

FIG. 3. Masses of $K^{\pm}$ mesons due to the interactions in the chiral SU(3) model at $T=0$, (i) without and (ii) with the contribution from the range term.

lar nucleon interaction term (the sigma term) [2] as well as the repulsive scalar contribution (proportional to the kinetic term of the pesudoscalar meson). The KN interaction is given as

$$\mathcal{L}_{KN} = -\frac{3i}{8f_K^2}\overline{N}\gamma^{\mu}N(K^-\partial_{\mu}K^+ - \partial_{\mu}K^-K^+) + \frac{\Sigma_{KN}}{f_K^2}(\overline{NN})K^-K^+ + \frac{\tilde{D}}{f_K^2}(\overline{NN})(\partial_{\mu}K^-)(\partial^{\mu}K^+). \quad (17)$$

where $\Sigma_{KN}=(\overline{m}+m_s/2)\langle N|(\overline{uu}+\overline{ss})|N\rangle$ [38]. In our calculations, we take $m_s=150$ MeV and $\overline{m}=(m_u+m_d)/2=7$ MeV.

The last term of the Lagrangian (17) is repulsive and is of the same order as the attractive sigma term. This, to a large extent, compensates the scalar attraction due to the scalar Σ term. The coefficient $\tilde{D}$ is fixed by the KN scattering lengths (see Ref. [39]) by choosing a value for Σ_{KN}, which depends on the strangeness content of the nucleon. Its value has, however, a large uncertainty. We consider the two extreme choices: $\Sigma_{KN}=2m_{\pi}$ and $\Sigma_{KN}=450$ MeV. The coefficient $\tilde{D}$, as fitted to the empirical value of the KN scattering length (16), is in general given by [39]

$$\tilde{D} \approx 0.33/m_K - \Sigma_{KN}/m_K^2. \quad (18)$$

In the next section, we shall discuss the results for the K-meson mass modification obtained in the effective chiral model as compared to chiral perturbation theory.

V. MEDIUM MODIFICATION OF K-MESON MASSES

We now investigate the K-meson masses in hot and dense hadronic medium within a chiral SU(3) model. The contributions from the various terms of the interaction Lagrangian (11) are shown in Fig. 1 in the mean-field approximation. The vector interaction as well as the ω exchange terms

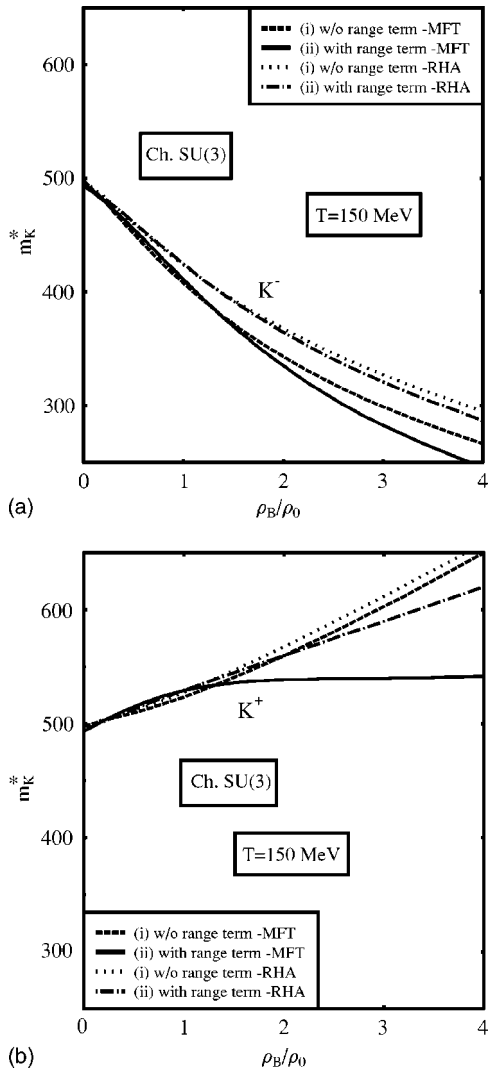

FIG. 4. Masses of $K^{\pm}$ mesons in the chiral SU(3) model for $T=150$ MeV, (i) without and (ii) with the range term contribution.

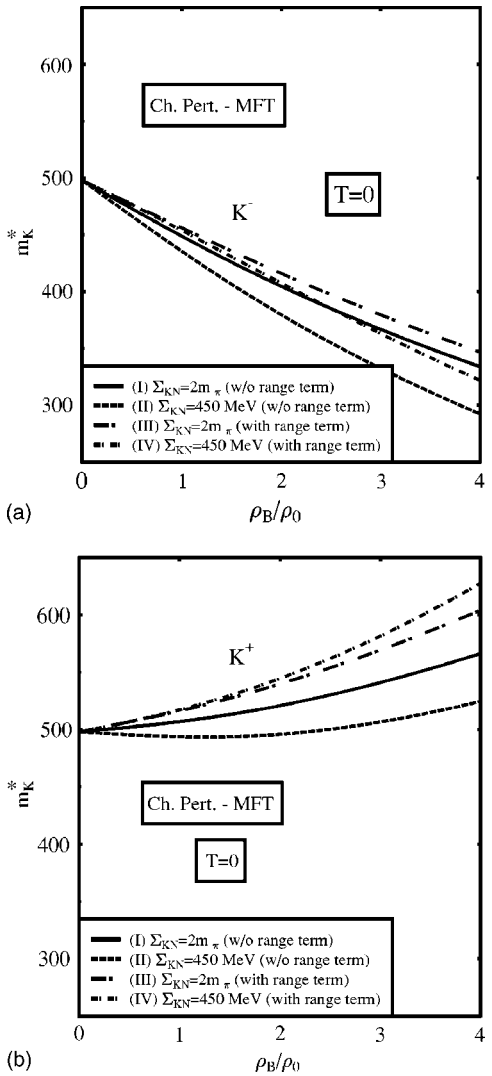

FIG. 5. Masses of $K^{\pm}$ mesons at $T=0$ in the mean-field approximation in chiral perturbation theory, without and with the contribution from the range term.

[given by the first and the third terms of Eq. (11), respectively] lead to a drop for the K^- mass, whereas they are repulsive for the K^+. The scalar meson exchange term is attractive for both K^+ and K^-. The first term of the range term of Eq. (11) is repulsive, whereas the second term has an attractive contribution. This results in a turnover of the K mass at around $0.8\rho_0$ above which the attractive range term [the last term in Eq. (11)] dominates. The dominant contributions arise from the scalar exchange and the range term (dominated by d_1 term at higher densities), which lead to a substantial drop of K-meson mass in the medium. The vector terms lead to a further drop of K^- mass, whereas for K^+ they compete with the contributions from the other two contributions. The effect from the nucleon Dirac sea on the mass modification of the K mesons is shown in Fig. 2. This gives rise to smaller modifications as compared to the mean-field calculations though qualitative features remain the same.

In Fig. 3 the masses of the K mesons are plotted for $T=0$ in the present chiral model. We first consider the situation when the Weinberg-Tomozawa term is supplemented by the scalar and vector meson exchange interactions [37]. The other case corresponds to the inclusion of the range terms in Eq. (11). Both the K-meson mass, as well as the $\bar{K}$ mass, drop at large densities when the range term is included.

In Fig. 4, the masses are plotted at a temperature of 150 MeV. The drop of the kaon masses are smaller as compared to the zero temperature case. This is due to the fact that the nucleon mass increases with temperature at finite densities in the chiral model used here [32,41]. Such a behavior of the nucleon mass with temperature was also observed earlier within the Walecka model by Ko and Li [41] in a mean-field calculation. The subtle behavior of the baryon self-energy can be understood as follows. The scalar self-energy in the mean-field approximation increases due to the thermal distribution functions at finite temperatures, whereas at higher temperatures there are also contributions from higher momenta which lead to lower values of the self-energy. These competing effects give rise to the observed increase of the effective baryon masses with temperature at finite densities. This change in the nucleon mass with temperature at finite density is also reflected in the vector meson (ω, ρ, and ϕ)

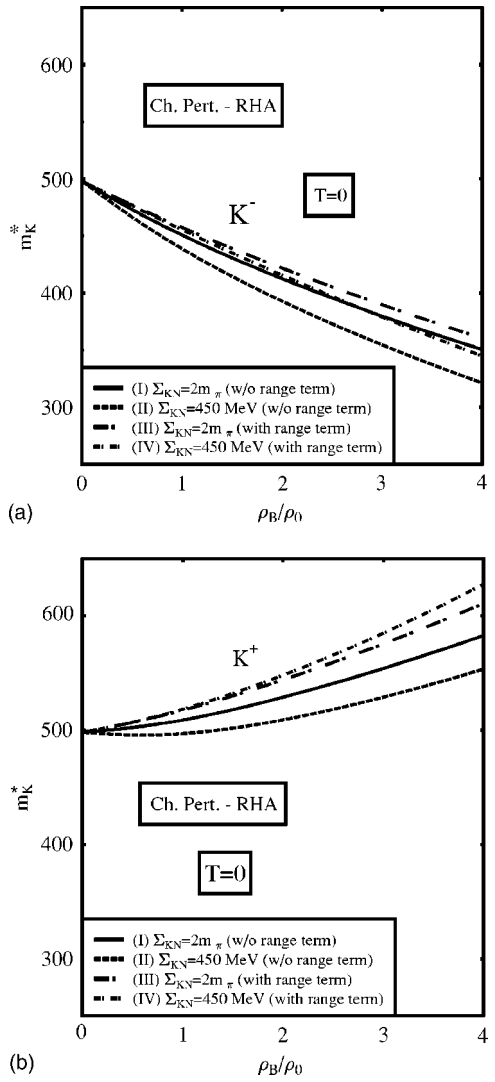

FIG. 6. Same as in Fig. 5, but in the relativistic Hartree approximation.

masses in the medium [32]. However at zero density, due to effects arising only from the thermal distribution functions, the masses are seen to drop continuously with temperature.

We compare the results obtained in the chiral effective model to those of the chiral perturbation theory (see Ref. [35,39]). The corresponding kaon masses are plotted in Figs. 5 and 6 at zero temperature for the mean field as well as for the relativistic Hartree approximation. The $K^{\pm}$ masses are plotted for different cases: (I) and (II) correspond to $\Sigma_{KN}=2m_{\pi}$ and $\Sigma_{KN}=450$ MeV, respectively, without the range term, while the cases (III) and (IV) are with the range term $(\partial_{\mu}K^{+})(\partial^{\mu}K^{-})$, with the parameter $\tilde{D}$ fitted to scattering length, so as to fulfill the low-density theorem [39]. The case (II) shows a stronger drop of the K^{-} mass in the medium as compared to the case (I) due to the larger attractive sigma term. For K^{+}, however, there are canceling effects from the sigma term and the Weinberg-Tomozawa interactions, leading to only a moderate mass modification. The inclusion of the repulsive range term in (III) and (IV) gives rise to a smaller drop of the K^{-} mass as compared to (I) and (II), respectively, where this term is absent. For K^{+}, the term gives higher values for the in-medium mass at large densities, as expected. The relativistic Hartree approximation shows again smaller mass modification as compared to the mean-field case. The K^{+}-meson mass shows a strong drop at large density in the chiral effective model as compared to the other approaches. The range term proportional to d_1 in Eq. (11) has to overcome the repulsive ω-exchange term, to be compatible with the KN scattering data, which is absent in chiral perturbation theory. This effect leads to a range term that is attractive contrary to the situation in chiral perturbation theory where the range term is repulsive. As a result, the effective chiral model gives stronger modifications for the K-meson masses as compared to chiral perturbation theory, especially at large density.

We note that the somewhat shallow attractive potential for K^{-} of -30 to -80 MeV at ρ_0 has been extracted also from coupled-channel calculations [17,24–27,29,30] when including effects from dressing the K^{-} propagator self-consistently.

VI. $K^{\pm}$ PRODUCTION AT SIS ENERGIES WITHIN A COVARIANT TRANSPORT MODEL

Since the different models discussed in the previous sections give very different results for the $K^{\pm}$ properties in the nuclear medium, it is of central importance to obtain further information from the experimental studies on $K^{\pm}$ production in order to support or reject part of the models. However, high-density matter can only be produced in relativistic nucleus-nucleus collisions, where $K^{\pm}$ production and propagation happens to a large extent out of kinetic and chemical equilibrium. One thus has to employ nonequilibrium transport approaches to follow the dynamics of all hadrons in phase space [42].

A. Description of the transport model

Our study of heavy-ion collisions is based on the hadron-string-dynamics (HSD) transport approach [13–15]. Though the HSD transport approach has been developed for the off-shell dynamic, including the propagation of hadrons with dynamical spectral functions [43], and also has been used in the context of K, $\bar{K}$ production and propagation in nucleus-nucleus collisions [16], we here restrict to the on-shell quasiparticle realization similar to Refs. [13–15]. The main reason is that the full off-shell calculations require the knowledge of the momentum, density, and temperature-dependent spectral functions of K, $\bar{K}$ mesons as well as the in-medium cross sections for all production and absorption channels. The latter have to be calculated in a consistent way, incorporating again the same spectral functions. Such information is naturally provided by coupled-channel G-matrix calculations [16]. However, the models presented in Secs. II–V are not suited for such purposes since they are formulated on the mean-field level, only. We note in passing that the differences between the present on-shell and the previous off-shell [16] versions of transport for $\bar{K}$ spectra in the SIS energy regime are less than 30% for the systems to be inves-

tigated below if similar antikaon potentials are employed [44].

In Refs. [13–15] the transition amplitudes for $\bar{K}N$ channels below the threshold of $\approx$1.432 GeV have been extrapolated from the vacuum amplitudes in an "ad hoc" fashion, which differ sizeably from more recent microscopic coupled-channel calculations [24–26,29]. To reduce this ambiguity we have adopted the results from the *G*-matrix calculations of Ref. [29], which have been also incorporated in the off-shell calculations [16] and extend far below the "free" threshold. The latter *G*-matrix calculations have been performed at a fixed temperature $T=70$ MeV, which corresponds to an average temperature of the "fireballs" produced in nucleus-nucleus collisions at SIS energies. We recall that variations in the temperature from 50–100 MeV do not sensibly affect the quasiparticle properties in the medium according to the studies in Ref. [29].

Actual cross sections in our present approach are determined as a function of the invariant energy squared s as [16]

$$\sigma_{1+2\to 3+4}(s) = (2\pi)^5 \frac{E_1E_2E_3E_4}{s}\frac{p'}{p}\int d\cos(\theta) \times \frac{1}{(2s_1+1)(2s_2+1)}\sum_i\sum_\alpha G^\dagger G, \quad (19)$$

where p and p' denote the center-of-mass momentum of the particles in the initial and final state, respectively, and E_j stand for the particle energies. The sums over i and α indicate the summation over initial and final spins, while s_1, s_2 are the spins of the particles in the entrance channel. Apart from the kinematical factors, the transition rates are determined by the angle integrated average transition probabilities

$$P_{1+2\to 3+4}(s) = \int d\cos(\theta)\frac{1}{(2s_1+1)(2s_2+1)}\sum_i\sum_\alpha G^\dagger G, \quad (20)$$

which, as mentioned above, are uniquely determined by the *G*-matrix elements evaluated for finite density ρ, temperature T, and relative momentum $p_{\bar{K}}$, with respect to the nuclear matter rest frame. The transition probabilities of Eq. (20) have been displayed in the right-hand side (r.h.s.) of Figs. 5–8 of Ref. [16] for the reactions $K^-p\to K^-p$, $K^-p\to\Sigma^0\pi^0$, $K^-p\to\Lambda\pi^0$, and $\Lambda\pi^0\to\Lambda\pi^0$ as a function of density and invariant energy, respectively. The latter have been parametrized by the authors of Ref. [16] and are available to the public [45]. In this context it is important to point out that the backward channels $K^-p\leftarrow\Sigma^0\pi^0$, $K^-p\leftarrow\Lambda\pi^0$, etc., are entirely determined by detailed balance, which is strictly fulfilled in the HSD transport approach using Eq. (19).

In principle, the real parts of the $\bar{K}$ self-energies are also fully determined by the *G*-matrix calculations. However, we here a adopt a *hybrid model* that keeps the in-medium transitions probabilities (20) fixed, and vary the real part of the $\bar{K}$ self-energies or antikaon potential according to the models presented in Secs. II–V. In this way one can study the explicit effect of the kaon and antikaon potentials in the nuclear medium in a more transparent way without employing too rough approximations for the transition probabilities involving antikaons. These transition amplitudes are beyond the level of mean-field theory essentially discussed in Secs. II–V.

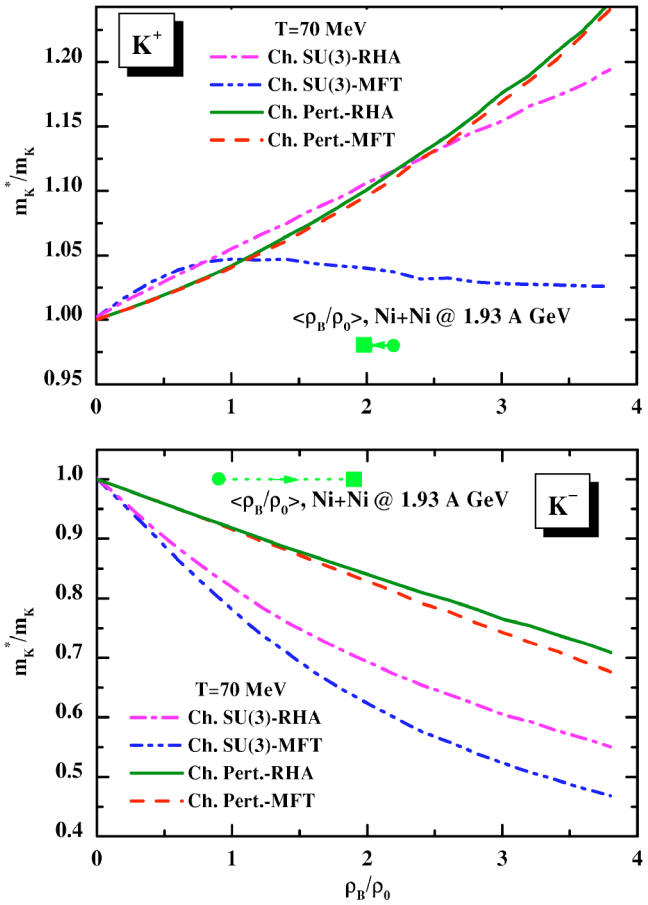

FIG. 7. (Color online) The ratio of the in-medium kaon (upper part) and antikaon (lower part) masses to the vacuum masses (m_K^*/m_K) as a function of baryon density in units of $\rho_0=0.16$ fm^{-3} calculated in the different models for the temperature $T=70$ MeV. The dotted-dashed lines correspond to the results within the chiral SU(3) model in the relativistic Hartree approximation [Ch. SU(3)-RHA], the dotted-dotted-dashed lines stand for the chiral SU(3) model in the mean-field approximation [Ch. SU(3)-MFT], the solid lines indicate the calculations within the chiral perturbation theory in relativistic Hartree approximation (Ch. Pert.-RHA) with the KN sigma term taken as 450 MeV, whereas the dashed lines show the results for the chiral perturbation theory in mean-field approximation (Ch. Pert.-MFT). The full symbols connected by arrows indicate the averaged freeze-out baryon density in units of ρ_0 of K^+ (upper part) and K^- mesons (lower part) for free (dots) and in-medium scenarios (squares) for central ($b=1$ fm) Ni+Ni collisions at 1.93*A* GeV.

We stress that for the present study we employ the kaon production cross sections for $N\Delta$ and $\Delta\Delta$ channels from Ref. [46] instead of the previously used fixed isospin relations, i.e., $\sigma_{N\Delta\to NKY}(\sqrt{s})=3/4\sigma_{NN\to NKY}(\sqrt{s})$ and $\sigma_{\Delta\Delta\to NKY}(\sqrt{s})=1/2\sigma_{NN\to NKY}(\sqrt{s})$. The kaon yields in vacuum now are on average enhanced by $\sim$30% relative to the yields in Refs. [13–15]. This enhancement is a consequence of the larger production cross section in the $N\Delta$ and $\Delta\Delta$ channels from Ref. [46] (as also used in Refs. [18,19]). Since these

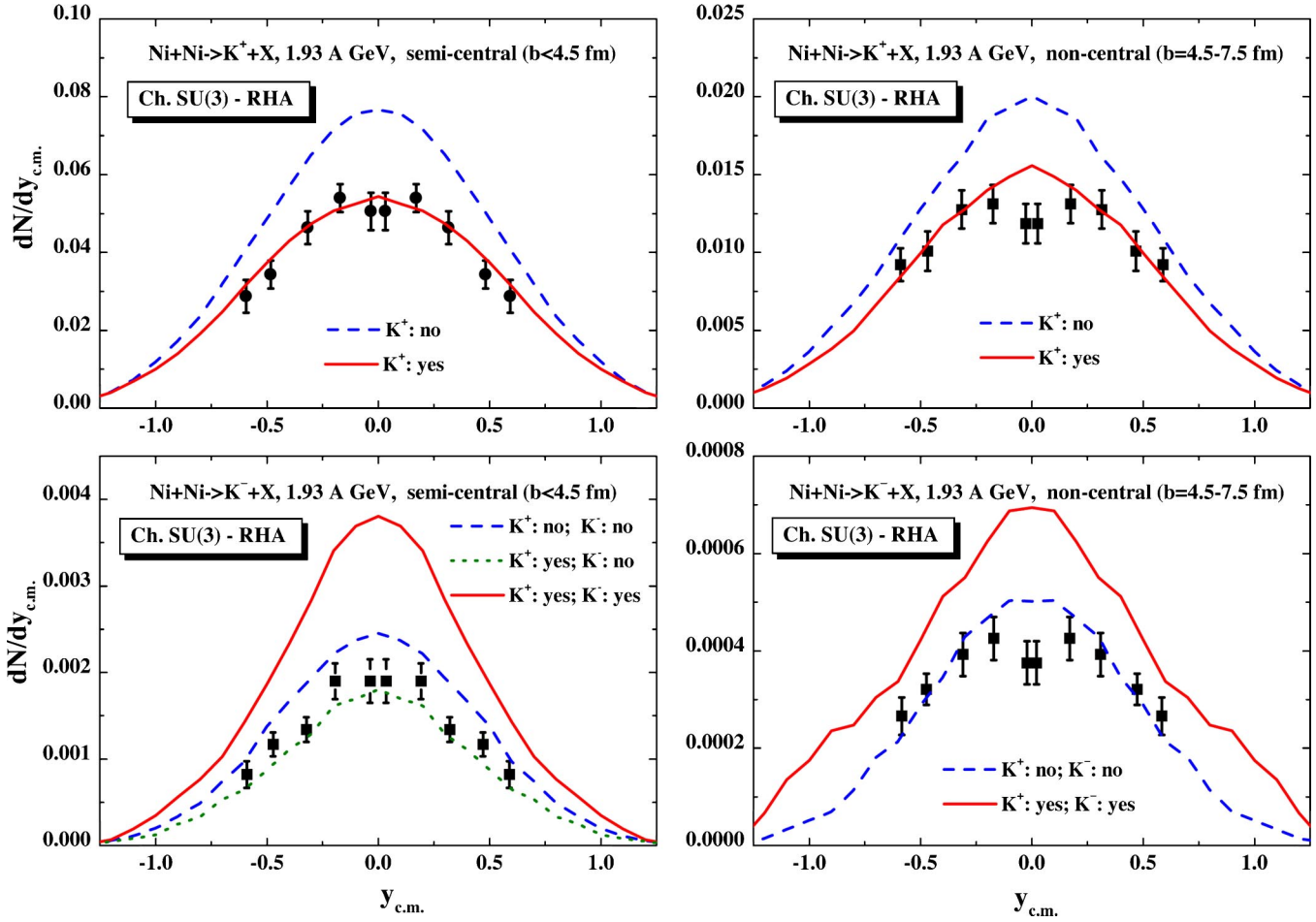

FIG. 8. (Color online) The rapidity spectra of K^+ (upper part) and K^- mesons (lower part) for Ni+Ni at 1.93A GeV for semicentral ($b \leqslant 4.5$ fm) (l.h.s.) and noncentral ($b=4.5-7.5$ fm) (r.h.s) collisions in comparison to the KaoS data from Ref. [5]. The dashed lines correspond to the free calculations, i.e., discarding K^+ and K^- potentials, the dotted line (lower left plot) shows the calculations with a K^+ potential according to the chiral SU(3)-RHA model, the solid lines correspond to the results for the K^+ and K^- potentials from the chiral SU(3)-RHA model.

resonance-induced production cross sections cannot be measured in vacuum, the actual K^+ yield from $A+A$ collisions calculated with transport models might differ substantially depending on the parametrizations involved.

B. $K^{\pm}$ spectra from nucleus-nucleus collisions

For reasons of transparency, we show in Fig. 7 the results from Secs. II–V for the kaon and antikaon masses in nuclear matter at a temperature $T=70$ MeV that are parametrized as a function of the density ρ_B and enter the transport calculation in the production as well as propagation parts. In Fig. 7 the dotted-dashed lines correspond to the results within the chiral SU(3) model in the relativistic Hartree approximation [Ch. SU(3)-RHA], the dotted-dotted-dashed lines stand for the chiral SU(3) model in the mean-field approximation [Ch. SU(3)-MFT], the solid lines indicate the calculations within the chiral perturbation theory in relativistic Hartree approximation (Ch. Pert.-RHA) with the KN sigma term taken as 450 MeV, whereas the dashed lines show the results for the chiral perturbation theory in mean-field approximation (Ch. Pert.-MFT). Whereas the results of the different models roughly coincide for kaons (upper part)—except for the limit Ch. SU(3)-MFT, the modifications of the K^- masses (lower part) differ more drastically. Here the Ch. SU(3)-MFT' limit gives the lowest masses, followed by Ch. SU(3)-RHA. The results from the two limits of chiral perturbation theory here provide the lowest mass modifications.

The full symbols connected by arrows indicate the averaged freeze-out baryon density in units of ρ_0 of K^+ (upper part) and K^- mesons (lower part) for free (dots) and in-medium scenarios (squares) for central ($b=1$ fm) Ni+Ni collisions at 1.93A GeV. Since K^+ mesons are basically produced from primary collisions and suffer less from rescattering, they see a higher baryon density $\sim 2\rho_0$. The K^- mesons are freezing-out later and dominantly stem from the pion-hyperon interactions [47]. Since the difference in the K^-N and $\pi\Lambda$ thresholds for the nonmodified K^- masses is about 320 MeV, the K^- mesons can be produced only by energetic pions or hyperons. Consequently, the density at the production point is only $\sim\rho_0$, i.e., lower than the initial baryon density achieved, e.g., in Ni+Ni collisions at 1.93A GeV. The in-medium shift of K^- masses reduces the thresholds for K^- production, such that K^- mesons are cre-

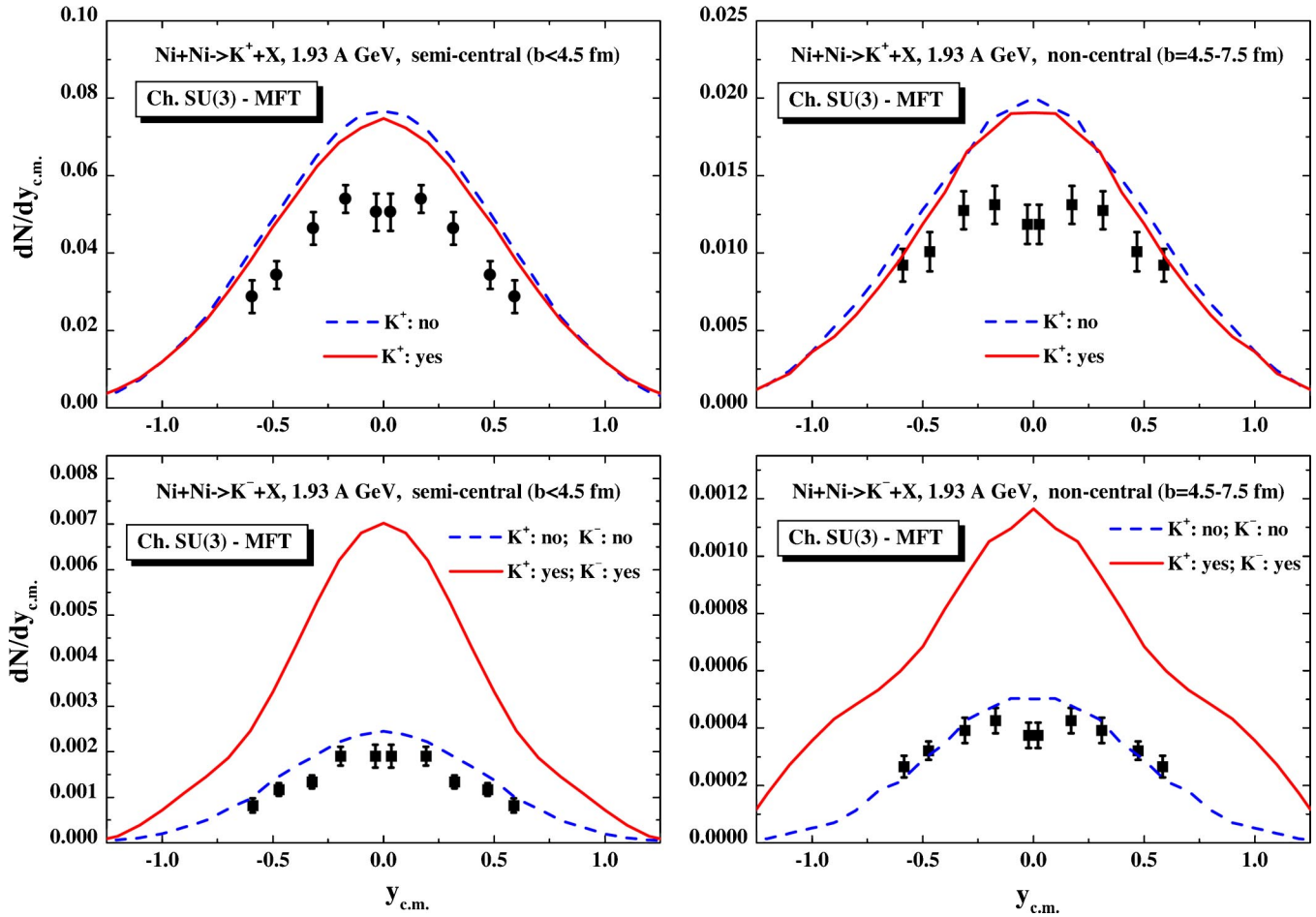

FIG. 9. (Color online) The rapidity spectra of K^+ (upper part) and K^- mesons (lower part) for Ni+Ni at 1.93*A* GeV for semicentral ($b \leqslant 4.5$ fm) (l.h.s.) and noncentral ($b=4.5-7.5$ fm) (r.h.s.) collisions in comparison to the KaoS data from Ref. [5]. The dashed lines correspond to the free'calculations, while the solid lines show the results for the K^+ and K^- potentials from the chiral SU(3)-MFT model.

ated earlier (and more frequently) by low-momentum particles at high baryon density $\sim 1.8\rho_0$ (depending on the strength of the attractive potential). Moreover, the in-medium absorption cross section of antikaons according to the transition probabilities employed here, is lower than the free absorption cross section.

Thus, K^+, K^- mesons produced in heavy-ion collisions probe the density regime $\sim 1-2\rho_0$, where the different models deviate substantially, so one can hope to check the reliability of the models by comparing to the experimental data for $A+A$ reactions.

We start with differential spectra for K^+ and K^- mesons from Ni+Ni reactions at 1.93*A* GeV for semicentral ($b \leqslant 4.5$ fm) [left-hand side (l.h.s.)] and noncentral ($b=4.5-7.5$ fm) (r.h.s) collisions in comparison to the KaoS data from Ref. [5] (Fig. 8). The dashed lines correspond to the "free" calculations, i.e., discarding K^+ and K^- potentials, the dotted line (lower left plot) shows the calculations with a K^+ potential according to the chiral SU(3)-RHA model, the solid lines correspond to the results for the K^+ and K^- potentials from the chiral SU(3)-RHA model. It is seen that the K^+ rapidity distributions are overestimated in comparison to the data when discarding a kaon potential. However, when including the repulsive K^+ potential from the chiral SU(3)-RHA model, a very satisfactory agreement is achieved for semicentral and noncentral collisions.

The K^- rapidity distributions are slightly overestimated when using only free kaon and antikaon masses. This limit, however, is unphysical since the K^+ spectra require a repulsive potential as demonstrated in the upper part of the figure. Now, when including the repulsive K^+ potential, the K^- rapidity distribution is slightly underestimated due to the lower amount of K^- production by the hyperon+pion production channel. Note, that the hyperon abundance is strongly correlated with the abundance of kaons due to strangeness conservation. Incorporating the very strong K^- potential from the chiral SU(3)-RHA model, however, the antikaon yields are severely overestimated by a factor of $\sim 1.6-1.8$. This result indicates that the attraction for the K^- in the chiral SU(3)-RHA model is too strong.

In Fig. 9 we show the same comparison as in Fig. 8 for the chiral SU(3)-MFT model. In this case the kaon potential is very low and practically does not give a sufficient reduction of the kaon rapidity distribution relative to the free case. Consequently, also the hyperon abundance is overestimated in this model, which gives too many antikaons (by the π +hyperon channels) already without indlucing any K potential. On the other hand, the chiral SU(3)-MET model leads to

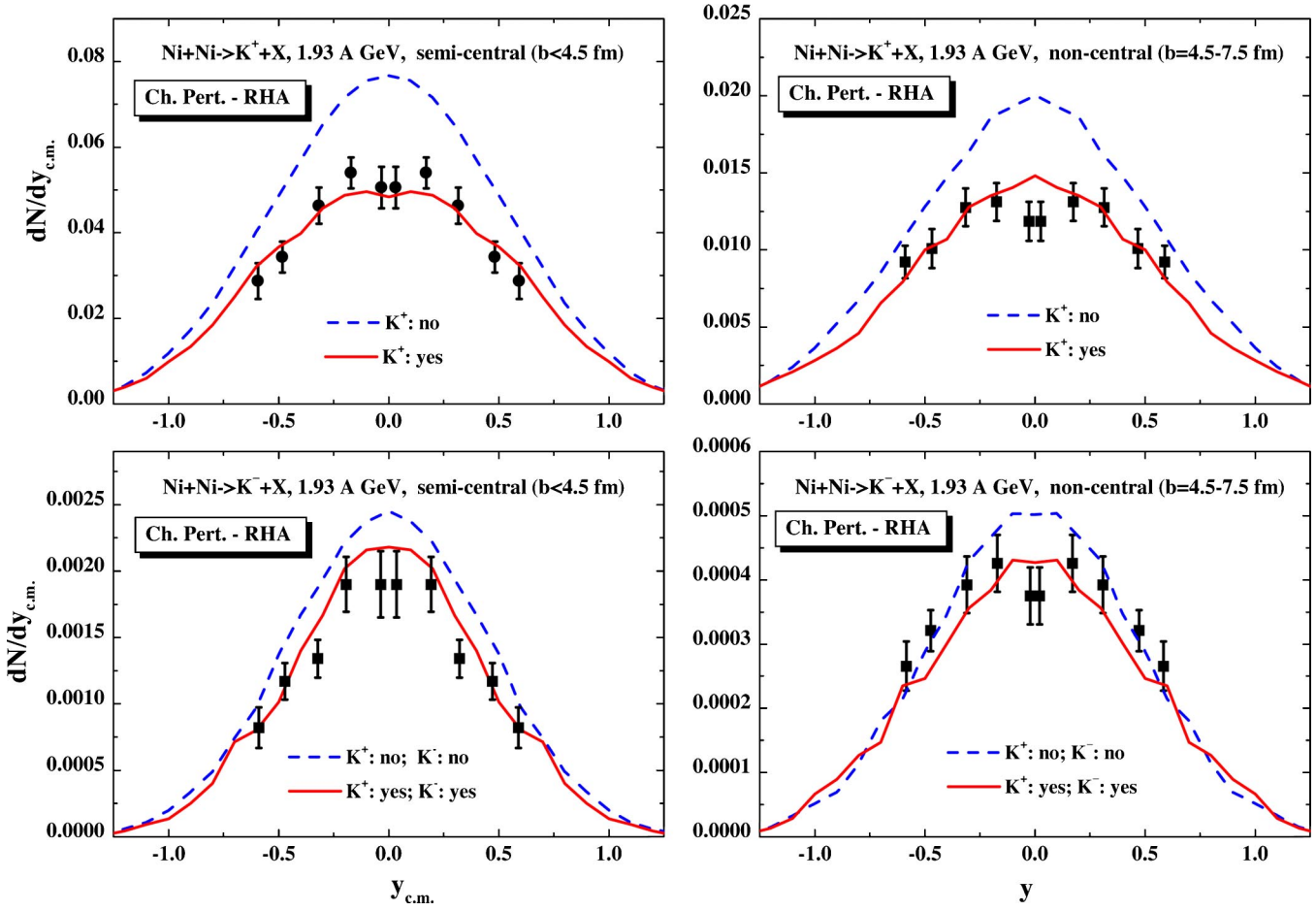

FIG. 10. (Color online) The rapidity spectra of K^+ (upper part) and K^- mesons (lower part) for Ni+Ni at 1.93*A* GeV for semicentral ($b \leqslant 4.5$ fm) (l.h.s.) and noncentral ($b=4.5-7.5$ fm) (r.h.s.) collisions in comparison to the KaoS data from Ref. [5]. The dashed lines correspond to the free'calculations, while the solid lines show the results for the K^+ and K^- potentials from the chiral perturbation theory in relativistic Hartree approximation (Ch. Pert.-RHA).

very strong K^- potentials which in turn give K^- yields in nucleus-nucleus collisions that are larger than the data by up to a factor of 3. We conclude that this model is essentially ruled out by the data due to (i) a lacking repulsion in the kaon channel and (ii) too much attraction in the antikaon channel.

In Fig. 10 we continue with the same comparison as in Fig. 8 for the Ch. Pert.-RHA. In this case the kaon potential potential is moderately repulsive and give a sufficient reduction of the kaon rapidity distribution relative to the free case almost perfectly in line with the data. When including now additionally the in-medium modifications, the K^- rapidity distributions are in a very good agreement with the data as in earlier studies such as Ref. [10]. We thus find that the chiral perturbation theory gives the proper repulsion in the kaon as well as attraction in the antikaon channel.

Though the Ni+Ni system at 1.93*A* GeV already provides clear hints for the proper size of $K^\pm$ self-energies at finite baryon density, it is important to check these indications by independent observables in a different system, too. In this respect we show in Fig. 11 the differential inclusive K^+ (upper part) and K^- spectra (lower part) for Au+Au at 1.48*A* GeV and $\theta_{\text{c.m.}}=(90\pm10)^o$ in comparison to the KaoS data from Ref. [7]. The dashed lines with open circles correspond to the free calculations, the dashed lines with open squares stand for the results with the K^+ and K^- potentials from the chiral SU(3)-RHA model, the dotted lines with open triangles indicate the calculations within the chiral SU(3)-MFT model and the solid lines with stars show the results with the K^+ and K^- potentials from chiral perturbation theory in relativistic Hartree approximation. We find that without any K^+ and K^- potentials the K^+ spectra are overestimated and show a slope parameter which is too low in comparison with experiment. Due to strangeness conservation also the hyperons are too frequent in this limit, which leads to a slight overestimation of the antikaon spectra. In this case the K^- slope comes out too high.

As discussed in the context of Fig. 9, the chiral SU(3)-MFT model yields only a small change of the K^+ spectra but overestimates the K^- spectra again by a factor of 3–4. Thus, we obtain the same conclusion for the Au+Au system at 1.48*A* GeV when looking at the transverse kinetic energy spectra. In the chiral SU(3)-RHA model the kaons come out reasonably well, but again the K^- spectrum is severely overestimated due to the strong attraction in the antikaon channel. Only the chiral perturbation theory (stars) provides a

good description of both spectra simultaneously, and also for the Au+Au system at 1.48*A* GeV, which gives a further indication for the proper $K^{\pm}$ self-energies given in this limit. We, furthermore, stress that not only the magnitude of the differential K^+, K^- spectra is described well in chiral perturbation theory, but also the K^+, K^- slopes (cf. Refs. [10,16]).

In Fig. 12 we show additionally the K^+ (upper part) and K^- angular distributions (lower part) for semicentral (l.h.s.) and noncentral (r.h.s.) Au+Au collisions at 1.48*A* GeV. We note that all angular distributions have been normalized to unity for $\cos\theta_{\mathrm{c.m.}}=0$ as well as the experimental data from Ref. [48]. The assignment of the individual lines from the different models is the same as in Fig. 11. We find that all models do not differ very much in the angular distributions that are more sensitive to the elastic and inelastic cross sections employed in the transport approach for kaons and antikaons. Only for noncentral collisions the K^- angular distribution comes out too flat in the free case, i.e., when no $K^{\pm}$ potentials and free transition rates for the scattering processes are used in the transport model. We note that these angular distributions are almost the same as in the full off-shell calculations from Ref. [16] for this system.

C. Collective flow of kaons and antikaons

Though the rapidity and transverse energy distributions for $K^{\pm}$ mesons have given some preference for chiral perturbation theory in the previous subsection, it is important to get independent information from further observables that are less sensitive to the explicit production cross sections from the various channels employed. We recall that especially the $K^{\pm}$ yields from $N\Delta$ and $\Delta\Delta$ channels are model dependent and cannot directly be measured in experiment. Futhermore, there are cancellation effects due to the different in-medium potentials for K^+ and K^-, which imply that the absolute magnitude of the spectra alone does not provide stringent information on the in-medium $K^{\pm}$ properties.

The collective flow of hadrons is experimentally defined by the anisotropy in the angular distribution as

$$\frac{dN}{d\phi} \sim 1 + 2v_1\cos(\phi) + 2v_2\cos(2\phi). \tag{21}$$

The coefficients v_1 and v_2 characterize directed and elliptic flow, respectively, and can be evaluated from the transport calculations as

$$v_1 = \left\langle \frac{p_x}{p_T} \right\rangle\Bigg|_{y,p_T}, \quad v_2 = \left\langle \frac{p_x^2 - p_x^2}{p_x^2 + p_y^2} \right\rangle\Bigg|_{y,p_T}, \tag{22}$$

where the beam is in z direction and the reaction plane oriented in x direction. An elliptic flow $v_2>0$ indicates in-plane emission of particles, whereas $v_2<0$ corresponds to a squeeze-out perpendicular to the reaction plane.

The elliptic flow v_2 is very sensitive to the strength of the interaction of K^+, K^- mesons with the nuclear environment. In the case of a repulsive potential (as for K^+) one expects $v_2<0$, i.e., a dominant out-of-plane emission of kaons due to the repulsive interaction with the nucleon spectators. Oppositely, for antikaons—which are attracted by the nucleon spectators—the coefficient v_2 is expected to be positive if the antikaon absorption by nucleon spectators is not too strong.

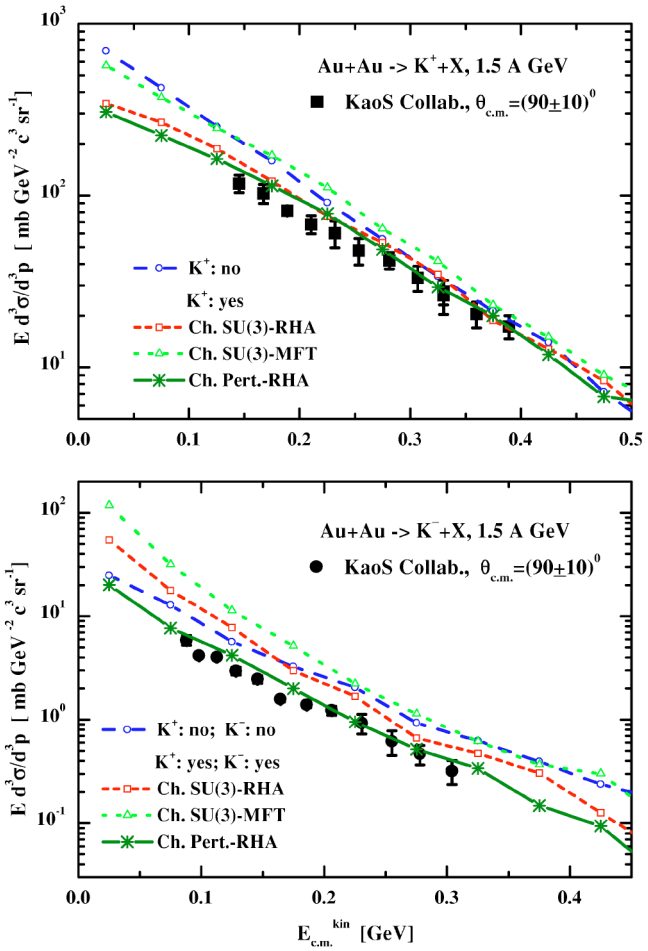

FIG. 11. (Color online) The differential inclusive K^+ (upper part) and K^- spectra (lower part) for Au+Au at 1.48*A* GeV and $\theta_{\mathrm{c.m.}}=(90\pm10)^{\circ}$ in comparison to the KaoS data from Ref. [7]. The dashed lines with open circles correspond to the 'free' calculations, the dashed lines with open squares stand for the results with the K^+ and K^- potentials from the chiral SU(3)-RHA model, the dotted lines with open triangles indicate the calculations within the chiral SU(3)-MFT model and the solid lines with stars show the results with the K^+ and K^- potentials from chiral perturbation theory in relativistic Hartree approximation.

Since the deviations from an isotropic angular distribution are small, one needs a transport calculation with very high statistics to extract solid numbers for the coefficients v_1 (or $\langle p_x\rangle$) and v_2 especially when gating additionally on rapidity y and/or the transverse momentum $p_T=\sqrt{p_x^2+p_y^2}$.

In Fig. 13 we show the $\langle p_x\rangle$ for K^+ (upper part) and K^- (lower part) mesons as a function of the normalized rapidity $y_{\mathrm{c.m.}}/y_{\mathrm{proj}}$ for Ni+Ni at 1.93*A* GeV. We have gated on central collisions ($b\leqslant 4$ fm) and applied a transverse momentum cut $p_T\geqslant 0.25$ GeV/c as for the experimental data of the FOPI Collaboration [49] (full dots). We find that when neglecting any potential for kaons and antikaons the $K^{\pm}$ flow follows the proton flow, however, with a lower magnitude. Since the kaon potential in the chiral SU(3)-MFT model is only very small, there is almost no change in $\langle p_x\rangle(y)$ (upper part) for

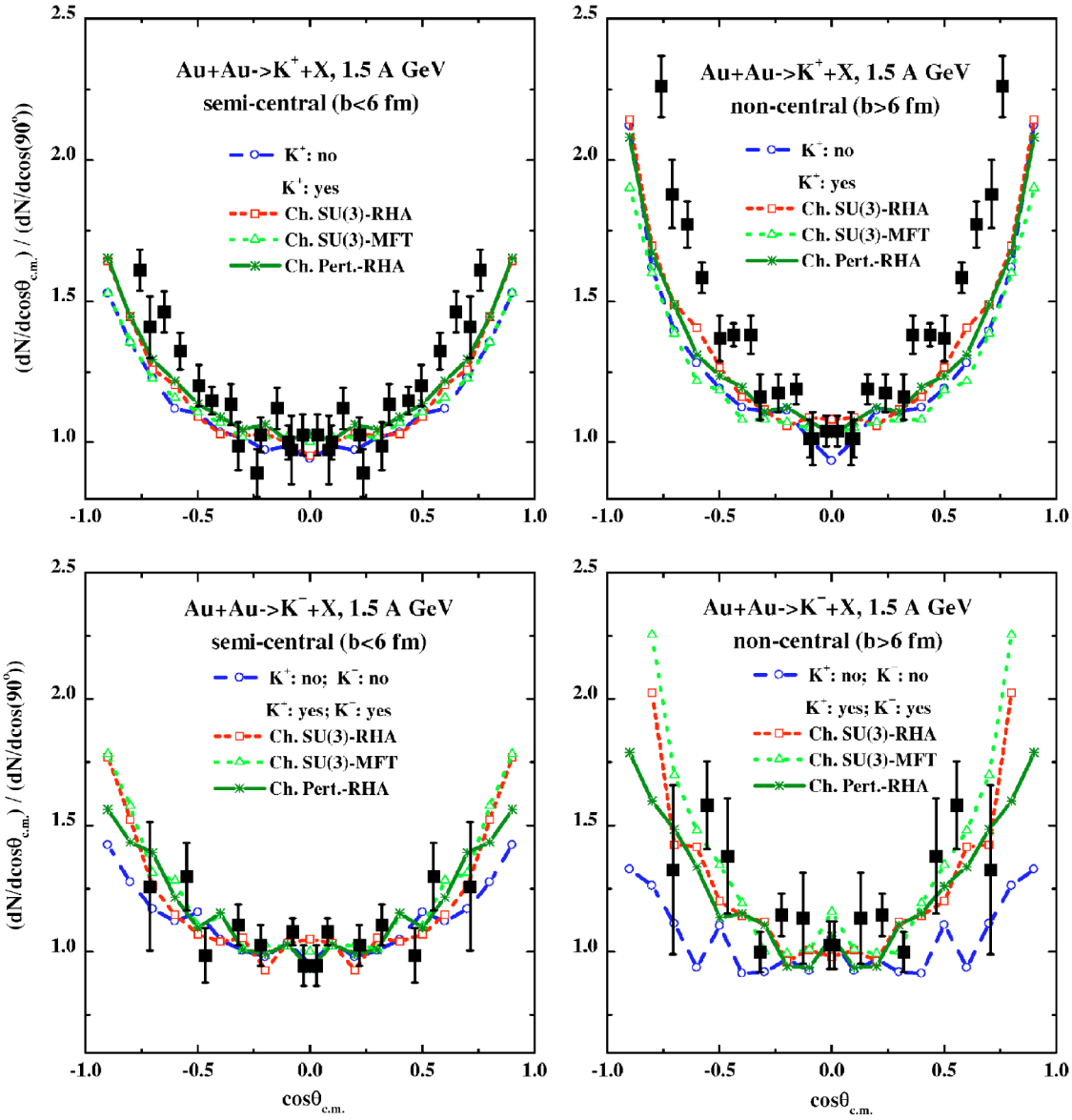

FIG. 12. (Color online) The K^+ (upper part) and K^- angular distributions (lower part) for semicentral (l.h.s.) and noncentral (r.h.s.) Au+Au collisions at 1.48*A* GeV. All angular distributions are normalized to unity for $\cos\theta_{\mathrm{c.m.}}=0$. The experimental data have been taken from Ref. [48]. The assignment of the individual lines is the same as in Fig. 11.

K^+ mesons. Only when including the moderate repulsive potential of the other models the kaons are "pushed away" from the protons and approximately show a vanishing (or even slightly opposite) flow pattern in line with the data. Consequently, the flow $\langle p_x\rangle(y)$ leads to the same conclusion on the kaon potential as in Sec. VI B, which is also consistent with the earlier studies in Refs. [10,15,20].

In contrast, the antikaons are attracted towards the proton flow direction by an attractive potential. This is most pronounced for the chiral SU(3)-MFT and -RHA models with their large attraction for antikaons. The results for the chiral perturbation theory, including a moderate K^- attraction, are in between the free and chiral SU(3) limits. Unfortunately, there are presently no comparable data to confirm or exclude the various models.

In Fig. 14 we, furthermore, provide predictions for the directed flow v_1 for K^+ (upper part) and K^- (lower part) mesons as a function of the center-of-mass rapidity $y_{\mathrm{c.m.}}$ for noncentral ($b=3.5-9.5$ fm) Ni+Ni collisions at 1.93*A* GeV. As it is well known, the flow phenomena are more pronounced for midcentral and peripheral nucleus-nucleus collisions; this is also seen from Fig. 14. Here the strong antiflow of K^+-mesons should allow us to further discriminate the models in the next round of experimental studies. This also holds for the strong attractive K^- flow in the lower part of Fig. 14 that needs experimental control.

In Figs. 15 and 16 we display the directed flow v_1 for K^+ (upper part) and K^- (lower part) mesons as a function of the transverse momentum p_T for noncentral ($b=3.5-9.5$ fm) Ni+Ni collisions at 1.93*A* GeV including the rapidity cut $0<y_{\mathrm{c.m.}}<0.5$. The p_T dependence of the v_1 is another observable that will allow for future experimental discrimination. Our calculations demonstrate that the kaon flow is practically zero if no potentials are employed. But for nonzero K^+

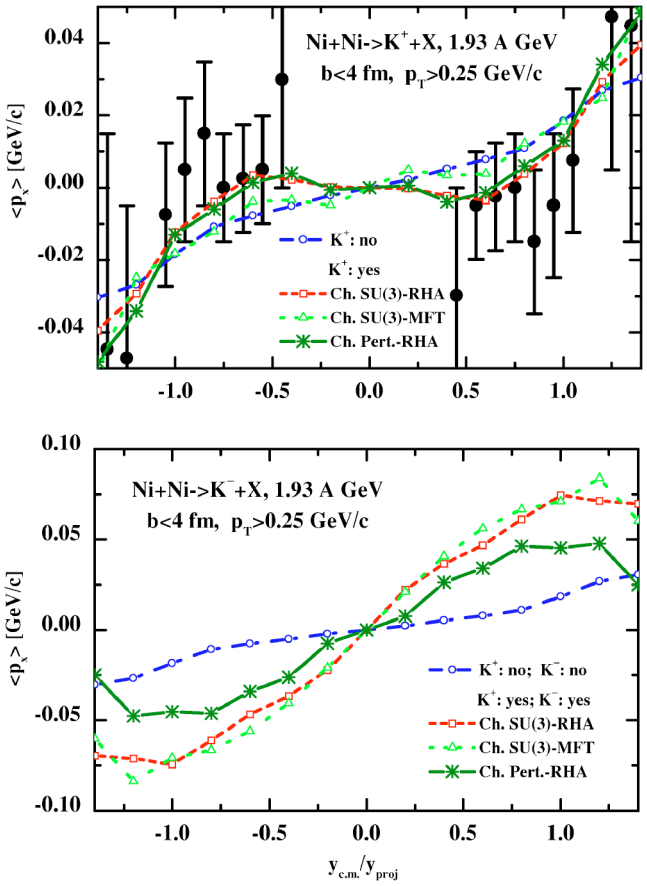

FIG. 13. (Color online) The $\langle p_x \rangle$ for K^+ (upper part) and K^- (lower part) mesons as a function of the normalized rapidity $y_{\mathrm{c.m.}}/y_{\mathrm{proj}}$ for Ni+Ni at 1.93*A* GeV. We have gated on central collisions ($b \leqslant 4$ fm) and applied a transverse momentum cut $p_T \geqslant 0.25$ GeV/c as for the experimental data of the FOPI Collaboration [49] (full dots). The assignment of the individual lines is the same as in Fig. 11.

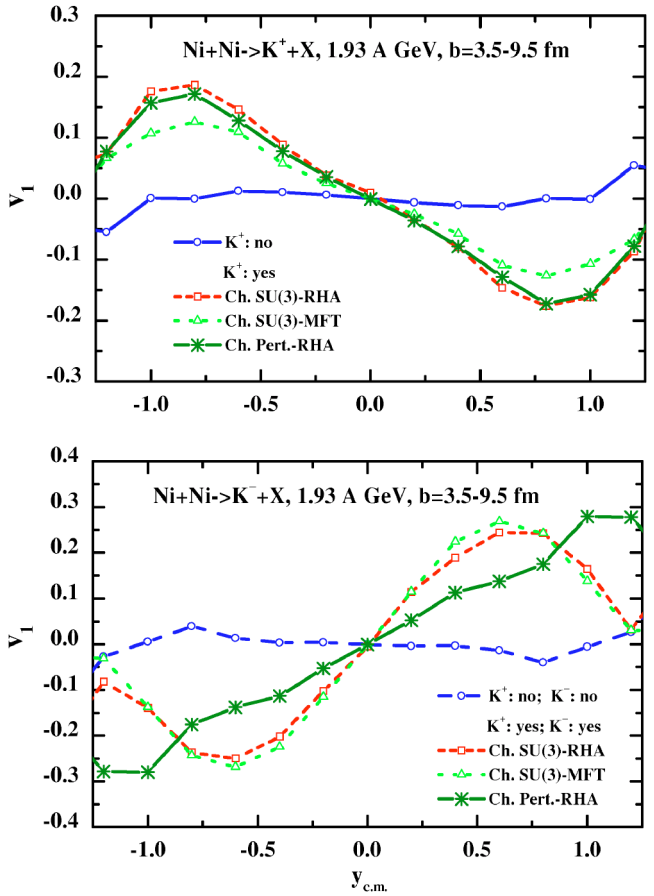

FIG. 14. (Color online) The directed flow v_1 for K^+ (upper part) and K^- (lower part) mesons as a function of the center-of-mass rapidity $y_{\mathrm{c.m.}}$ for noncentral ($b=3.5-9.5$ fm) Ni+Ni collisions at 1.93*A* GeV. The assignment of the individual lines is the same as in Fig. 11.

potentials, v_1 becomes increasingly negative with p_T up to $p_T \approx 0.4$ GeV/c. The strength of v_1 is, furthermore, almost proportional to the strength of the kaon self-energy. The antikaons show a qualitatively similar behavior in p_T, but with the opposite sign. There is practically no signal—within statistics—for a nonvanishing v_1 when discarding a K^- potential. Only when including moderate (for the chiral perturbation theory) or stronger antikaon potential [for the chiral SU(3)-RHA and -MFT models] a positive signal in v_1 is found again, which is most pronounced for momenta in the 0.2–0.4 GeV/c regime.

We finally present our results for the elliptic flow v_2 for K^+ (upper part) and K^- (lower part) mesons as a function of the center-of-mass rapidity $y_{\mathrm{c.m.}}$ for noncentral ($b=3.5-9.5$ fm) Ni+Ni collisions at 1.93*A* GeV. The calculations show a distinct dependence of the elliptic flow as a function of the rapidity in the c.m. system ($y_{\mathrm{c.m.}}$) for kaons as well as antikaons. For K^+ mesons the flow is always negative, i.e., enhanced perpendicular to the reaction plane. The size of this "squeeze-out," however, provides a measure for the strength of the repulsive potential. For free antikaons the elliptic flow is again compatible with zero (within statistics), but directed in-plane for all rapidities when including attractive potentials. These effects are small at midrapidity, but become more pronounced for $|y_{\mathrm{c.m.}}| > 0.5$, where the spectator nucleons show up. Also note that the $K^{\pm}$ mesons in the interactions with spectators only probe densities $\rho_B \leqslant \rho_0$. The next round of experiments should allow to put some further constraints on the models.

We stress that there is a clear difference for free and in-medium K^+, K^- scenarios in the v_1 (or $\langle p_x \rangle$), v_2 flow patterns which provides a unique signal for medium modifications. Thus, future experiments with sufficient statistics might be able not only to confirm unambiguously medium effects for K^+ and K^- mesons, but also provide constraints on the underlying potentials in a dense and hot medium.

VII. SUMMARY

To summarize, we have investigated in a chiral SU(3) model the temperature and density dependence of the $K, \bar{K}$-meson masses arising from the interactions with nucleons and scalar and vector mesons. The properties of the light hadrons—as studied in a SU(3) chiral model—modify the *K*-meson properties in the hot and dense hadronic medium.

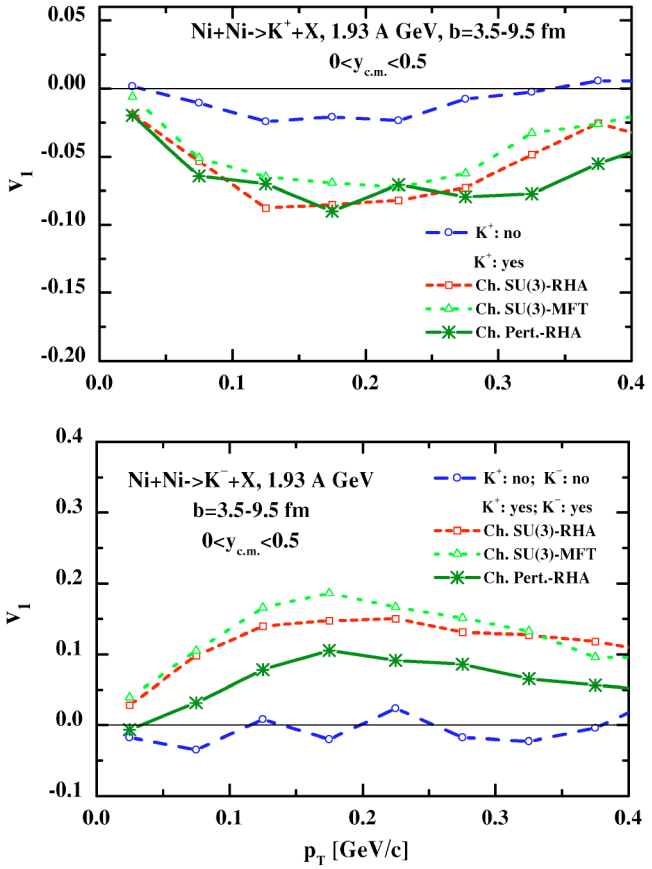

FIG. 15. (Color online) The directed flow v_1 for K^+ (upper part) and K^- (lower part) mesons as a function of the transverse momentum p_T for noncentral ($b=3.5-9.5$ fm) Ni+Ni collisions at 1.93A GeV including the rapidity cut $0<y_{\mathrm{c.m.}}<0.5$. The assignment of the individual lines is the same as in Fig. 11.

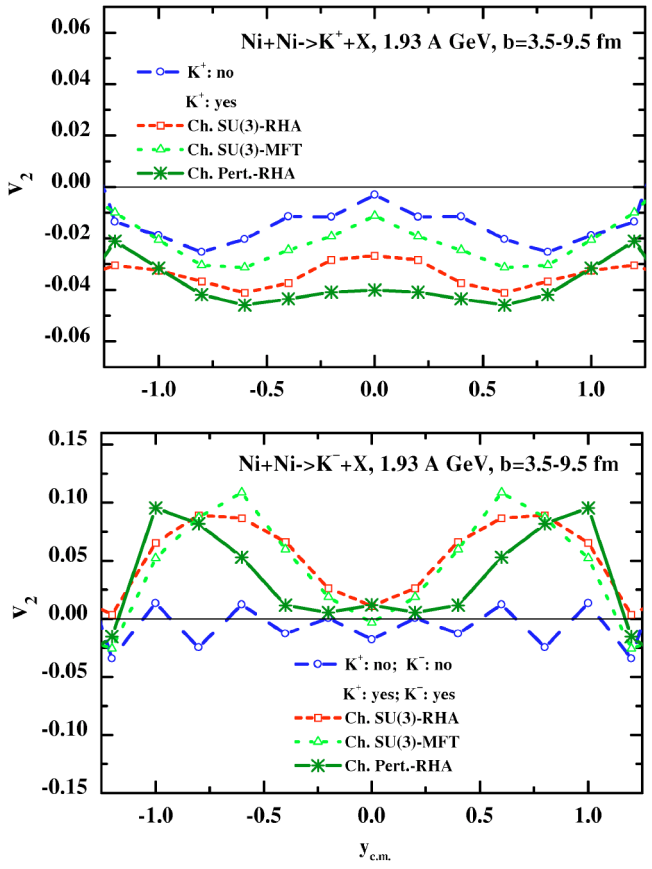

FIG. 16. (Color online) The v_2 coefficient for K^+ (upper part) and K^- (lower part) mesons as a function of the center-of-mass rapidity $y_{\mathrm{c.m.}}$ for noncentral ($b=3.5\div9.5$ fm) Ni+Ni collisions at 1.93A GeV. The assignment of the individual lines is the same as in Fig. 11.

The SU(3) model with parameters fixed from the properties of hadron masses, nuclei and hypernuclei and KN scattering data, takes into account all terms up to the next to leading order arising in chiral perturbative expansion for the interactions of K mesons with baryons. The important advantage of the present approach is that the DN, KN as well as πN Σ terms are calculated within the model itself. The predictions for the πN and KN Σ terms are reasonable, the value for Σ_{KN} from the model being, furthermore, in agreement with lattice gauge calculations.

Using the Lagrangian from chiral perturbation theory with a Tomozawa-Weinberg interaction, supplemented by an attractive scalar interaction (the Σ term) for the KN interactions, the results obtained are seen to be similar to earlier calculations: the K^+ mass increases with density while the K^- mass decreases. However, the presence of the repulsive range term, given by the last term in (17), reduces the drop in the antikaon mass. The chiral effective model, which is adjusted to describe nuclear properties, gives a larger drop of the K-meson masses at finite density as compared to chiral perturbation theory dominantly due to an attractive range term. Furthermore, the effect of the baryon Dirac sea for hot hadronic matter [within the chiral SU(3) model] gives a slightly higher value for the K-meson masses as compared to the mean-field calculations, while the qualitative trends in the medium remain.

Since the predictions of the various models differ substantially for the $K^{\pm}$ masses at finite density and temperature we have used a covariant transport approach to study the potential effects of the models in comparison to experimental data at SIS energies. Our detailed analysis for $K^{\pm}$ rapidity and transverse energy distributions has given a clear preference for the potentials from chiral perturbation theory, which yields a moderately repulsive kaon potential and a moderately attractive antikaon potential. We stress that this moderate K^- potential is in agreement with more sophisticated coupled-channel calculations, which take into account effects from the $\Lambda(1405)$ and dress the in-medium K^- propagator selfconsistently.

As pointed out in Sec. V, the effective SU(3) chiral model gives stronger modifications for the K-meson masses as compared to chiral perturbation theory, especially at large density, due to the repulsive ω-exchange term, which is absent in chiral perturbation theory. This effect leads to a range term which is attractive contrary to the situation in chiral perturbation theory where the range term is repulsive. In the absence of the ω-exchange term in the chiral SU(3) model, however, the qualitative features can be similar in both models.

One has to keep in mind also, that the SU(3) model has been constructed in order to describe nuclear properties at normal baryon density. Moreover, it is a "static" theory since it is formulated on the mean-field level only, i.e. dynamical effects such as momentum dependence of the kaon/antikaon potentials are not included. Our analysis shows that the heavy-ion data indicate that such a restricted picture of in-medium effects doesn't work at high baryon densities. Moreover, it seems quite difficult to constrain the parameters of the chiral SU(3) model such that they describe the heavy-ion data and simultaneously achieve a good agreement with the nuclear matter data. Most likely, more sophisticated scenarios as coupled-channel *G*-matrix calculations provide a more realistic picture of the medium modification of kaons and antikaons.

We have, furthermore, calculated the collective flow for kaons and antikaons in Ni+Ni reactions at 1.93*A* GeV, which shows a clear dependence on the strength of the potentials for non-central and peripheral collisions. Moreover, the dependence of the flow coefficients v_1 and v_2 on the transverse momentum p_T and on the rapidity y show a sensitivity to the sign and magnitude of the $K^{\pm}$ potentials. These sensitivities can be used to determine the in-medium properties of the kaons and antikaons from the experimental side in the near future [50].

ACKNOWLEDGMENTS

We thank H. Oeschler, J. Reinhardt, P. Senger, L. Tolós, and F. Uhlig for fruitful discussions and W. Cassing for the actual version of the HSD transport code used in our analysis. One of the authors (A.M.) is grateful to the Institut für Theoretische Physik Frankfurt for the warm hospitality. A.M. acknowledges financial support from Bundesministerium für Bildung und Forschung (BMBF) and ELB from Deutsche Forschungsgemeinschaft (DFG) and GSI. The support from the Frankfurt Center for Scientific Computing (CSC) is additionally gratefully acknowledged.

[1] Proceedings of Quark Matter 2002 [Nucl. Phys. **A715**, 1 (2003)].
[2] D. B. Kaplan and A. E. Nelson, Phys. Lett. B **175**, 57 (1986); A. E. Nelson and D. B. Kaplan, *ibid.* **192**, 193 (1987).
[3] D. Best *et al.*, FOPI Collaboration, Nucl. Phys. **A625**, 307 (1997).
[4] F. Laue *et al.*, KaoS Collaboration, Phys. Rev. Lett. **82**, 1640 (1999).
[5] M. Menzel *et al.*, KaoS Collaboration, Phys. Lett. B **495**, 26 (2000).
[6] C. Sturm *et al.*, KaoS Collaboration, Phys. Rev. Lett. **86**, 39 (2001).
[7] A. Förster *et al.*, KaoS Collaboration, J. Phys. G **28**, 2011 (2002).
[8] X. S. Fang, C. M. Ko, G. Q. Li, and Y. M. Zheng, Phys. Rev. C **49**, R608 (1994); G. Q. Li, C. M. Ko, and X. S. Fang, Phys. Lett. B **329**, 149 (1994).
[9] C. M. Ko and G. Q. Li, J. Phys. G **22**, 1673 (1996); C. M. Ko, V. Koch, and G. Q. Li, Annu. Rev. Nucl. Part. Sci. **47**, 505 (1997).
[10] G. Q. Li, C.-H. Lee, and G. E. Brown, Nucl. Phys. **A625**, 372 (1997).
[11] C. M. Ko, J. Phys. G **27**, 327 (2001).
[12] S. Pal, C. M. Ko, and Z.-W. Lin, Phys. Rev. C **64**, 042201 (2001).
[13] W. Cassing, E. L. Bratkovskaya, U. Mosel, S. Teis, and A. Sibirtsev, Nucl. Phys. **A614**, 415 (1997).
[14] E. L. Bratkovskaya, W. Cassing, and U. Mosel, Nucl. Phys. **A622**, 593 (1997).
[15] W. Cassing and E. L. Bratkovskaya, Phys. Rep. **308**, 65 (1999).
[16] W. Cassing, L. Tolós, E. L. Bratkovskaya, and A. Ramos, Nucl. Phys. **A727**, 59 (2003).
[17] J. Schaffner-Bielich, V. Koch, and M. Effenberger, Nucl. Phys. **A669**, 153 (2000).
[18] C. Hartnack, H. Oeschler, and J. Aichelin, Phys. Rev. Lett. **90**, 102302 (2003).
[19] C. Fuchs, Amand Faessler, E. Zabrodin, and Yu-Ming Zheng, Phys. Rev. Lett. **86**, 1974 (2001); C. Fuchs, nucl-th/0312052.
[20] G. Q. Li, C. M. Ko, and B. A. Li, Phys. Rev. Lett. **74**, 235 (1995); Nucl. Phys. **A594**, 460 (1995); G. Q. Li and C. M. Ko, Phys. Rev. C **54**, 1897 (1996); G. Q. Li, C. M. Ko, and G. E. Brown, Phys. Lett. B **381**, 17 (1996).
[21] G. E. Brown and M. Rho, Phys. Rev. Lett. **66**, 2720 (1991).
[22] E. Friedman, A. Gal, and C. J. Batty, Nucl. Phys. **A579**, 518 (1994).
[23] A. Gal, Nucl. Phys. **A691**, 268 (2001).
[24] M. Lutz, Phys. Lett. B **426**, 12 (1998).
[25] M. Lutz and E. E. Kolomeitsev, Nucl. Phys. **A700**, 193 (2002).
[26] M. Lutz and C. L. Korpa, Nucl. Phys. **A700**, 309 (2002).
[27] A. Ramos and E. Oset, Nucl. Phys. **A671**, 481 (2000).
[28] V. Koch, Phys. Lett. B **337**, 7 (1994).
[29] L. Tolós, A. Ramos, and A. Polls, Phys. Rev. C **65**, 054907 (2002).
[30] L. Tolós, A. Ramos, A. Polls, and T. T. S. Kuo, Nucl. Phys. **A690**, 547 (2001).
[31] P. Papazoglou, D. Zschiesche, S. Schramm, J. Schaffner-Bielich, H. Stöcker, and W. Greiner, Phys. Rev. C **59**, 411 (1999).
[32] A. Mishra, K. Balazs, D. Zschiesche, S. Schramm, H. Stöcker, and W. Greiner, Phys. Rev. C **69**, 024903 (2004).
[33] D. Zschiesche, A. Mishra, S. Schramm, H. Stöcker, and W. Greiner, nucl-th/0302073.
[34] A. Mishra, E. Bratkovskaya, J. Schaffner-Bielich, S. Schramm, and H. Stöcker, Phys. Rev. C **69**, 015202 (2004).
[35] J. Schaffner-Bielich, I. N. Mishustin, and J. Bondorf, Nucl. Phys. **A625**, 325 (1997).
[36] J. J. Sakurai, *Currents and Mesons* (University of Chicago Press, Chicago, 1969).
[37] G. Mao, P. Papazoglou, S. Hofmann, S. Schramm, H. Stöcker, and W. Greiner, Phys. Rev. C **59**, 3381 (1999).

[38] G. E. Brown and M. Rho, Phys. Rep. **269**, 333 (1996).
[39] G. E. Brown, C.-H. Lee, M. Rho, and V. Thorsson, Nucl. Phys. **A567**, 937 (1994).
[40] T. Barnes and E. S. Swanson, Phys. Rev. C **49**, 1166 (1994).
[41] G. Q. Li, C. M. Ko, and G. E. Brown, Nucl. Phys. **A606**, 568 (1996).
[42] W. Cassing and U. Mosel, Prog. Part. Nucl. Phys. **25**, 235 (1990).
[43] W. Cassing and S. Juchem, Nucl. Phys. **A665**, 377 (2000); *ibid.* **A672**, 417 (2000); *ibid.* **A677**, 445 (2000).
[44] W. Cassing (private communication).
[45] W. Cassing, http://theorie. physik. uni-giessen. de/~cassing/downloads
[46] K. Tsushima *et al.*, Phys. Rev. C **59**, 369 (1999).
[47] C. M. Ko, Phys. Lett. **120**, 294 (1983).
[48] A. Förster, *et al.*, KaoS Collaboration, Phys. Rev. Lett. **91**, 152301 (2003).
[49] N. Herrmann *et al.*, FOPI Collaboration, Nucl. Phys. **A610**, 49c (1996); B. Hong *et al.*, Phys. Rev. C **57**, 244 (1998).
[50] P. Senger (private communication).